Supporting Information for:

H_2-driven biocatalytic *O*-demethylation of lignin derived aromatics in a closed-loop flow system powered by water electrolysis

Donato Calabrese[†,a], Guiyeoul Lim[†,a], Parsa Nayyara[b], Megan E. Wolf[b], Paul R. F. Cordero[a], Lindsay D. Eltis[b,*] and Lars Lauterbach[a,b,c,*]

[a]*Institute of Applied Microbiology – iAMB, RWTH Aachen University, Worringer Weg 1, Aachen 52074, Germany.*
[b]*Department of Microbiology and Immunology, Life Sciences Institute, BioProducts Institute, The University of British Columbia, 2350 Health Sciences Mall, Vancouver, V6T 1Z3, Canada.*
[c]*Fraunhofer Institute for Molecular Biology and Applied Ecology IME, Forckenbeckstr. 6, 52074 Aachen, Germany.*

† These authors have contributed equally to this work
*Corresponding authors

Table of Contents

1 Chemicals and Materials

Catalase was purchased from TCI chemicals (Japan). Ethylguaiacol, ethylcatechol, methoxybenzoic acid, hydroxybenzoic acid, vanillic acid and protocatechuic acid were purchased from Sigma-Aldrich (Germany). Buffer components were bought from SERVA (Germany). Chemicals for media preparations and dialysis membrane (5 kDa) were obtained from Carl Roth GmbH (Germany). Peristaltic pump (Reglo ICC) was purchased from IDEX (USA). Portable spectrophotometer (Model Genova Bio, Jenway) was bought from Cole-Parmer (USA). O_2 adhesive spot sensor was purchased from PreSens (Germany). H_2 sensor was purchased from Unisense (Denmark). Mini flow cuvette was obtained from Hellma analytics (Germany). PEM electrolyzer (E206, 65) was obtained from H-TEC education. Teflon (OD 2 mm, ID 1.5 mm, length 2 m), tubing was bought from CS-Chromatographie Service GmbH (Germany). Fluran® tubing was purchased from VWR (Germany). Amberlite resin was obtained from Rohm & Haas (USA). C 10/10 Column was purchased from Cytiva (USA).

2 Strains and Plasmids

Table S1: Strains used in this study

Strain	Use	Source
E. coli BL-21 λ (DE3)	Protein expression	Invitrogen
E. coli DH5α	DNA propagation	Invitrogen

Table S2: Plasmids used in this study

Plasmid	Description	Source
pET28a	*E. coli* expression vector, kanamycin resistance	Novagen
pET15b	*E. coli* expression vector, ampicillin resistance	Novagen
pET28a_*pbdA*	pET28a harboring *pbdA* from RHA1	This study
pET28a_*hapux*	pET28a harboring *RPB_3614* from *R. palustris* HaA2	This study
pET28a_*hapur*	pET28a harboring *RPB_3656* from *R. palustris* HaA2	This study
pET15b_*agcA*	pET15b harboring *agcA* from EP4	[1]
pET15b_*agcB*	pET15b harboring *pbdA* from EP4	[1]
pET28a_*vanA*	pET28a harboring *vanA* from KT2440	[2]
pET28a_*vanB*	pET28a harboring *vanB* from KT2440	[2]

3 Experimental Section

3.1 Preparation of proteins

AgcA

Cell cultures of *E. coli* Bl21 (DE3) containing the pET15a_agcA plasmid were grown in LB medium with ampicillin (100 µg/mL) at 37 °C and 200 rpm until an OD_{600} of 1.0 was reached. Expression was induced by adding IPTG to a final concentration of 0.1 mM, and the cultures were incubated for 16–18 h at 30 °C. After harvesting the cells by centrifugation at 5,000 × *g* for 30 min at 4 °C, the pellets were stored at -80 °C. The frozen pellets were resuspended in lysis buffer (20 mM KPO_4, pH 8.0, 300 mM KCl, 10 mM imidazole) at 5 mL per gram of cell pellet. Lysis was performed using a Constant Systems Cell Disruptor at 18,000 psi, and the lysate was clarified by centrifugation at 12,000 × *g* for 60 min at 4 °C. The cleared lysate was loaded onto a Ni-NTA column pre-equilibrated with lysis buffer. The column was washed with 10 CVs of wash buffer (20 mM KPO_4, pH 8.0, 300 mM KCl, 25 mM imidazole) and eluted with 5 column volumes (CVs) of elution buffer (20 mM KPO_4, pH 8.0, 300 mM KCl, 250 mM imidazole). Purified protein was subjected to heme reconstitution by adding a 50 mM hemin solution in 0.1 M NaOH dropwise (1–3 molar equivalents of heme per protein). Reconstitution was monitored via UV-Vis spectroscopy, ensuring a Soret peak ratio (R_0) > 1.1. The protein was concentrated using a 30 kDa MWCO centrifugal filter, exchanged into 20 mM KPO_4, pH 8.0, and stored at -80 °C.

AgcB

Cell cultures of E. coli Bl21 (DE3) containing the pET15a_agcB plasmid were grown in LB medium containing ampicillin (100 µg/mL) at 37 °C with shaking at 200 rpm until an OD_{600} of 0.6. Expression was induced by adding IPTG to a final concentration of 0.1 mM, along with Fe(III) ammonium citrate (10 µM final concentration) to promote proper folding. The cultures were incubated for 24 h at 16 °C. Cells were harvested by centrifugation at 5,000 × *g* for 30 min at 4°C, and the pellets were stored at -80 °C. Lysis and purification were performed in an anaerobic glovebox to maintain oxygen-free conditions. The frozen pellets were resuspended in lysis buffer (20 mM KPO_4, pH 8.0, 300 mM KCl, 10 mM imidazole) and lysed using a Constant Systems Cell Disruptor at 18,000 psi. The lysate was clarified by centrifugation at 12,000 × *g* for 60 min at 4 °C. Ni-NTA purification was conducted as described for AgcA, except for the use of anaerobic conditions throughout. The protein was concentrated, exchanged into 20 mM KPO_4, pH 8.0, and stored anaerobically at -80 °C.

PbdA

Cell cultures of E. coli Bl21 (DE3) containing the pET28A_pbdA plasmid were grown in LB medium with kanamycin (50 µg/mL) at 37 °C and 200 rpm until reaching an OD_{600} of 1.0. IPTG was added to a final concentration of 0.3 mM, and the cultures were incubated for 16–18 h at 30 °C. Cells were harvested by centrifugation at 5,000 × *g* for 30 min at 4 °C, and pellets were stored at -80 °C. The pellets were resuspended in lysis buffer (20 mM Tris-HCl, pH 8.0, 300 mM KCl, 10 mM imidazole) and lysed using a Constant Systems Cell Disruptor at 18,000 psi. After clarification by centrifugation (12,000 × *g*, 60 min, 4 °C), Ni-NTA purification was performed using lysis, wash (25 mM imidazole), and elution (250 mM imidazole) buffers. Heme reconstitution was carried out by adding hemin as described for AgcA, with a target R_0 > 1.8. The protein was concentrated, exchanged into 20 mM Tris-HCl, pH 8.0, and stored at -80 °C.

HaPuX

Cell cultures of E. coli Bl21 (DE3) containing the pET28A_hapux plasmid were grown in LB medium supplemented with kanamycin (50 µg/mL) at 37 °C with shaking until reaching an OD_{600} of 1.0. IPTG was added to a final concentration of 0.3 mM, and Fe(III) ammonium citrate (10 µM final concentration) was added at induction. The cultures were incubated for 16–18 h at 23 °C. Cells were

lysed and purified following the same protocol as PbdA, with iron incorporation validated via UV-Vis spectroscopy. The protein was concentrated, exchanged, and stored at -80 °C.

HaPuR

Cell cultures of E. coli Bl21 (DE3) containing the pET28A_hapur plasmid were grown in LB medium with kanamycin (50 µg/mL) at 37 °C until reaching an OD_{600} of 1.0. IPTG was added to a final concentration of 0.3 mM, and the cultures were incubated for 16–18 h at 23 °C. Harvested cells were processed using the same lysis and purification protocols as PbdA. The purified protein was concentrated, exchanged into 20 mM Tris-HCl, pH 8.0, and stored at -80 °C.

VanA

Cell cultures of E. coli Bl21 (DE3) containing the pET28A_vanA plasmid were grown in LB medium supplemented with kanamycin (50 µg/mL) at 37 °C with shaking until reaching an OD_{600} of 1.0. At this point, IPTG was added to a final concentration of 0.3 mM, and $FeCl_3$ (10 µM final concentration) was added to promote proper iron incorporation during protein folding. The cultures were incubated for 16–18 h at 20 °C. Cells were harvested by centrifugation at 5,000 × *g* for 30 min at 4 °C, and the resulting pellets were stored at -80 °C. The pellets were resuspended in lysis buffer (20 mM HEPPS, pH 8.0, 300 mM KCl, 10 mM imidazole) and lysed using a Constant Systems Cell Disruptor at 18,000 psi. The lysate was clarified by centrifugation at 12,000 × *g* for 60 min at 4 °C. Ni-NTA purification was performed by loading the lysate onto a column equilibrated with lysis buffer, washing with 10 CVs of wash buffer (20 mM HEPPS, pH 8.0, 300 mM KCl, 25 mM imidazole), and eluting with 5 CVs of elution buffer (20 mM HEPPS, pH 8.0, 300 mM KCl, 250 mM imidazole). The eluted protein was concentrated using a 30 kDa MWCO centrifugal filter, exchanged into storage buffer (20 mM HEPPS, pH 8.0), and stored at -80 °C.

VanB

Cell cultures of *E. coli* BL21 (DE3) containing the pET28A_vanB plasmid were grown in LB medium supplemented with kanamycin (50 µg/mL) at 37 °C with shaking until reaching an OD_{600} of 1.0. IPTG was added to a final concentration of 0.3 mM, and $FeCl_3$ (10 µM final concentration) was added at induction to promote proper iron incorporation. The cultures were incubated for 16–18 h at 20 °C. Cells were lysed and purified following the same protocol as VanA, with Ni-NTA purification performed using wash buffer containing 40 mM imidazole. The purified protein was validated for iron incorporation via UV-Vis spectroscopy, concentrated, exchanged into storage buffer (20 mM HEPPS, pH 8.0), and stored at -80 °C.

Soluble hydrogenase (SH)

SH from *Cupriavidus necator* was produced homologously in *C. necator* cells harboring the pGE771 plasmid. Cultivation was carried out heterotrophically in mineral salts medium supplemented with 0.05% (w/v) fructose, 0.4% (v/v) glycerol, 1 µM $NiCl_2$, 40 µM $FeCl_3$, 1 µM $ZnCl_2$, and trace elements. Cultures were grown in 5 L Erlenmeyer flasks containing 4 L of medium to limit oxygen transfer. The flasks were incubated at 120 rpm until an optical density at 436 nm (OD_{436}) of approximately 11 was reached. Cells were harvested by centrifugation at 6,000 × *g* for 30 min at 4 °C. The harvested cells were resuspended in 50 mM potassium phosphate, pH 7.0, containing 5% glycerol, 5 mM NAD^+, and an EDTA-free protease inhibitor cocktail (Roche) at a buffer-to-cell ratio of 3:1 (v/w). To minimize protein oxidation, the resuspension and subsequent steps were performed under an argon atmosphere. The suspension was degassed with argon prior to cell disruption using a cooled French press operated at 18,000 psi. During lysis, an argon overlay was applied to the French press chamber to further ensure an oxygen-free environment. The lysate was clarified by ultracentrifugation at 100,000 × *g* for 45 min at 4 °C, with the supernatant maintained under an argon overlay throughout to preserve the integrity of the soluble proteins. Purification of SH was conducted using affinity

chromatography on a Strep-Tactin Superflow column (IBA). The clarified lysate was loaded onto the column under an argon overlay to protect the protein from oxygen exposure. The column was washed sequentially with 5 CVs of the resuspension buffer and 10 CVs mL of the same buffer lacking NAD^+. The bound SH protein was eluted using NAD^+-free buffer supplemented with 5 mM desthiobiotin, with all steps carried out under an argon atmosphere. Eluted fractions containing SH were pooled and concentrated using an Amicon Ultra-15 centrifugal filter unit (100 kDa MWCO, Merck Millipore). Throughout purification, the use of argon overlay ensured minimal oxygen exposure to protect the SH protein's activity. After concentration, the buffer was exchanged into storage buffer (20 mM Tris-HCl, pH 8.0), and stored at -80 °C.

3.2 Batch reactions with varying gas composition

3.2.1 Detailed methods

Batch reactions were conducted in 8 mL gas-tight vials to ensure precise control over gas compositions throughout the experiments. Each vial contained 1 mL of reaction mixture, prepared in 20 mM phosphate, pH 8.0 and composed of 1 mM NAD^+, 10 mM substrate, and enzyme concentrations tailored to each system. Substrates were chosen based on the specificity of the enzymatic systems: 4-ethylguaiacol (CAS 2785-89-9) for AgcAB, 4-methoxybenzoate (CAS 100-09-4) for PbdA/HaPuXR, and vanillate (CAS 121-34-6) for VanAB. Enzyme concentrations were adjusted as follows: 5 µM for AgcA and AgcB, 10 µM for VanA and VanB; 10 µM for PbdA; 5 µM for HaPuX; 1 µM for HaPuR; and 2.5 µM for soluble hydrogenase (SH). Gas compositions were prepared using a gas mixing station, calibrated to deliver mixtures of H_2, O_2, and N_2 at a total flow rate of 100 mL/min. Oxygen concentration was fixed at 20%, while hydrogen concentrations were varied from 2% to 20% in increments of 2%, with nitrogen as the balancing gas. The prepared gas mixture was delivered to each vial through a dual-needle setup: one needle introduced the gas mixture into the vial, while a second allowed the internal air to escape, ensuring no pressure build-up. The input needle was submerged directly into the liquid phase, allowing the gas to bubble through the reaction mixture for 5 min, facilitating efficient gas exchange with the solution. To maintain the integrity of the headspace composition, the needles were removed sequentially, starting with the output needle, immediately after the bubbling process. The vials were sealed with gas-tight butyl rubber septa and aluminum caps. Enzymes were added to the reaction mixture using a gas-tight syringe (Hamilton Company), ensuring no contamination of the gas composition during this step. The reactions were incubated at 30°C with continuous shaking at 200 rpm to ensure proper mixing. After 16 h of incubation, 50 µL samples were taken from each reaction mixture and quenched with an equal volume of 100% acetonitrile. The quenched samples were placed on ice before analysis. Substrate conversion and product formation were quantified using high-performance liquid chromatography (HPLC) with UV detection. The analysis was performed using a Macherey-Nagel NUCLEODUR C18 Gravity column (75 mm length, 4.6 mm inner diameter, 3 µm particle size). The solvent system started at 95% water + 0.1% formic acid and gradually shifted to 95% acetonitrile over a 20-min gradient. The flow rate was set to 1 mL/min, and UV readings were taken at 254 nm, 280 nm, 290 nm, and 320 nm. This method allowed for the resolution of all analytes present in the reaction mixtures. Conversion rates were determined by comparing the peak areas of the samples against those of standard compounds analyzed under the same HPLC conditions. Negative controls, including vials without enzymes or substrates, were processed in parallel to account for potential non-enzymatic background reactions.

3.2.2. Additional Results and HPLC Chromatograms

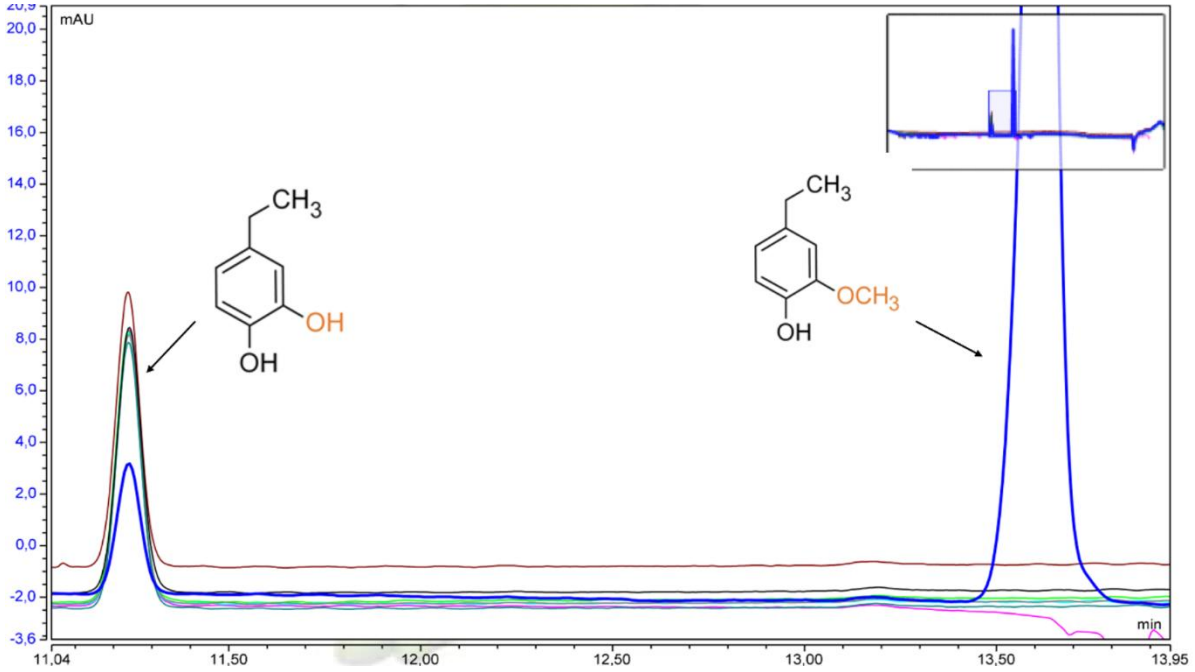

Fig. S1. Chromatograms of AgcAB/SH reactions performed using different concentration of H_2. illustrating the conversion of ethylguaiacol (**1a**) to ethylcatechol (**1b**) by AgcAB under varying gas compositions. The blue trace represents the reaction with 2% H_2, while other traces correspond to reactions conducted at higher H_2 concentrations.

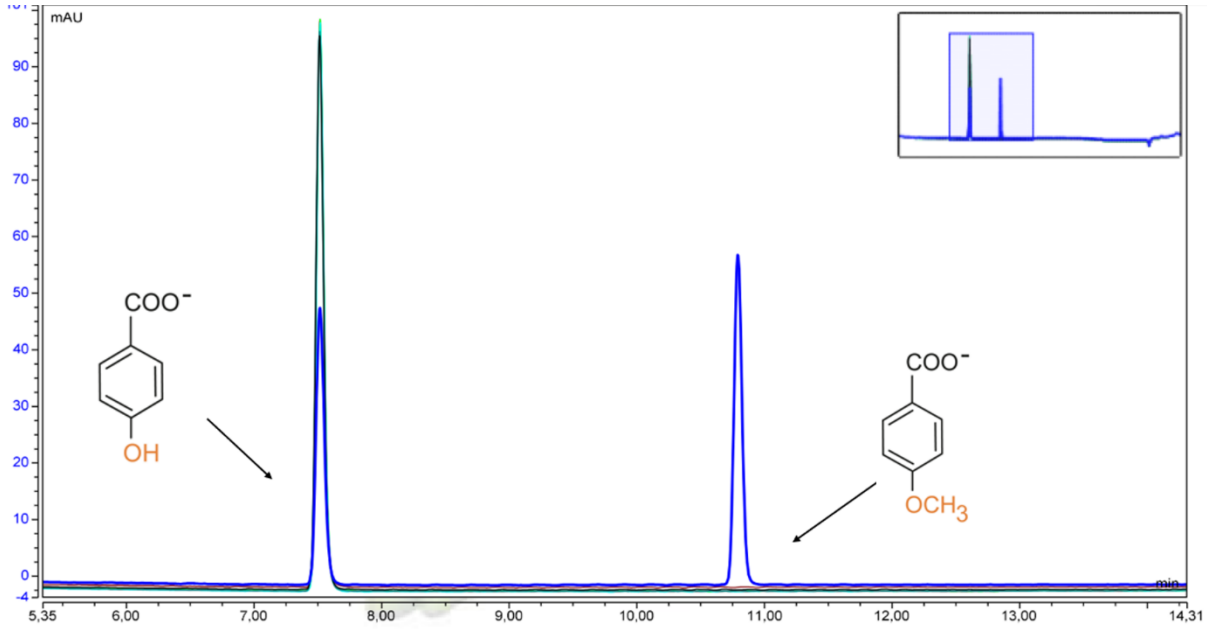

Fig. S2. Chromatograms of PbdA/HaPuXR/SH reactions performed using different concentration of H_2. illustrating the conversion of p-methoxybenzoate (**2a**) to hydroxybenzoate (**2b**) by PbdA/HaPuXR under varying gas compositions. The blue trace represents the reaction with 2% H_2, while other traces correspond to reactions conducted at higher H_2 concentrations.

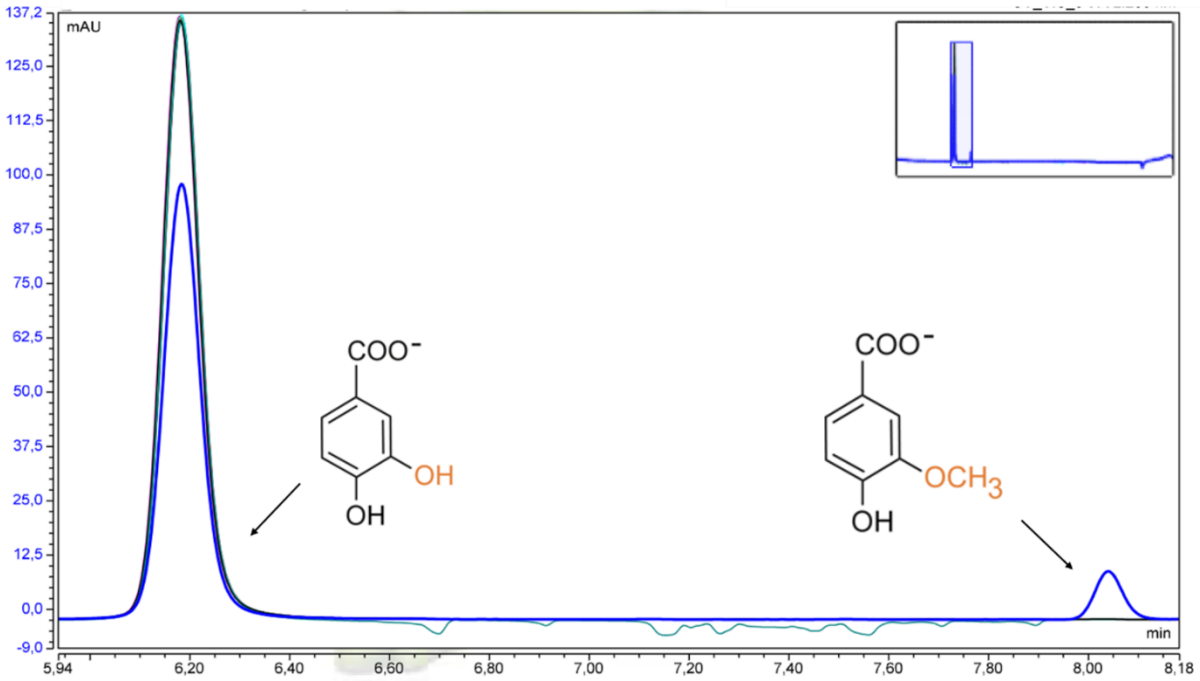

Fig. S3. Chromatograms of VanAB/SH reactions performed using different concentration of H_2. illustrating the conversion of vanillate (**3a**) to protocatechuate (**3b**) by VanAB under varying gas compositions. The blue trace represents the reaction with 2% H_2, while other traces correspond to reactions conducted at higher H_2 concentrations.

3.2.3 Optimization of the H_2/O_2 Composition

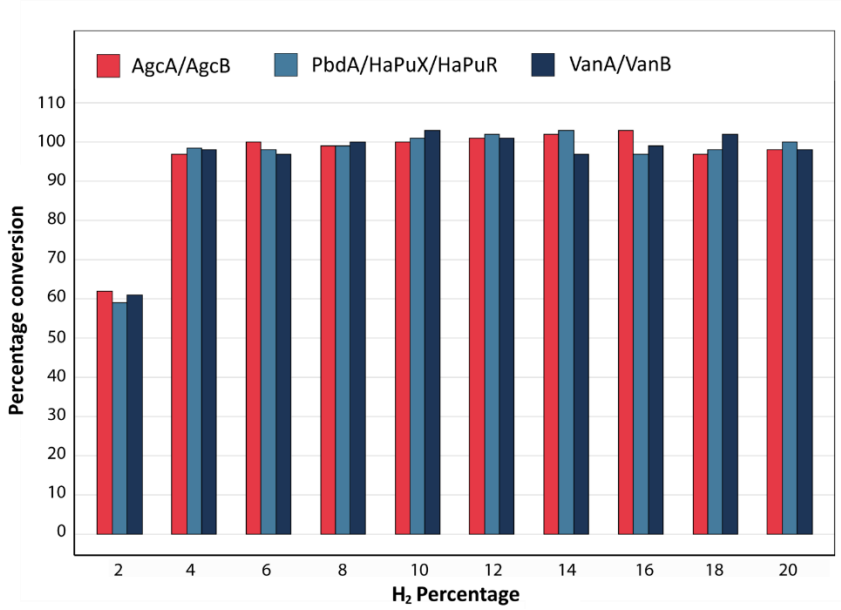

Fig. S4. Effect of H_2 Concentration on Product Yields of AgcAB, PbdA/HaPuXR, and VanAB with SH-Mediated Cofactor Regeneration. Product yields of AgcAB, PbdA/HaPuXR, and VanAB were measured under varying H_2 concentrations (2–20%) at constant O_2 (20%) using SH-mediated NADH regeneration. Batch reactions were conducted in 8 mL gas-tight vials (1 mL reaction volume) in 20 mM phosphate, pH 8.0, containing 1 mM NAD^+ and 10 mM substrate. Substrates were **1a** for AgcAB,

2a for PbdA/HaPuXR, and **3a** for VanAB. Enzyme concentrations were 5 µM for AgcA and AgcB, 10 µM for VanA and VanB, 10 µM for PbdA, 5 µM for HaPuX, 1 µM for HaPuR, and 2.5 µM for SH.

3.3 PbdA/HaPuXR coupling studies

Table S3: Coupling efficiency of PbdA with the artificial electron transfer system HaPuX/HaPuR

PbdA:HaPux:HaPuR	Rate of product formation [$U/\mu M_{P450}$]	Rate of NADH consumption [$U/\mu M_{P450}$]	Coupling [%]
1 : 0.5 : 0.3	14	26	53
1 : 0.2 : 0.3	5.2	14	35
1 : 0.1 : 0.3	4.6	16	29
1 : 0.5 : 0.1	35	34	103
1 : 0.2 : 0.1	14.7	18	80
1 : 0.1 : 0.1	9.3	11	85
1 : 1 PbdAB*	24.3 (0.9)	24 (3)	100 (3)

* From Wolf et al., 2024 [3]

For activity measurements PbdA, HaPux and HapuR were combined in a 200 µL cuvette in Tris-Cl (pH 7.4, 50 mM ionic strenght) with substrate diluted in the same buffer. 350 µM of NADH was added to initiate the reaction. For HPLC analysis, enzymatic reactions were acidified by adding acetic acid to 10% final concentration, centrifuged (16,000 × *g* for 10 min), and filtered through a 0.2 µm PTFE membrane. Samples were run over a Luna 5 µm C18(2) 100 Å 150 × 3 mm column (Phenomenex) at 0.7 mL min^{-1} by a Waters 2695 separation HPLC module. Samples were eluted with a 16.8 mL linear gradient from 1% methanol plus 0.1% formic acid in water to 100% methanol plus 0.1% formic acid and monitored at 280_{nm} with a Waters 2996 photodiode array detector. Concentrations were determined by interpolation on a standard curve of 0 to 1 mM of authentic standard. NADH concentration was measured by absorbance at 340_{nm}, ε = 6.22 $mM^{-1}cm^{-1}$. Coupling was calculated from the ratio of rate of aromatic turnover, as determined by HPLC, and the rate of NADH oxidation, determined spectroscopically.

3.4 H_2-driven batch O-demethylations and HPLC analysis

3.4.1 Detailed Methods

Batch reactions for studying H_2-driven O-demethylations were performed in 8 mL gas-tight vials, each containing 1 mL of reaction mixture prepared in 20 mM phosphate, pH 8.0, with 0.1 – 0.4 mM NAD^+, 10 mM substrate, and enzyme concentrations optimized for each system. Ethylguaiacol served as the substrate for AgcA and AgcB, methoxybenzoate for PbdA, HaPuX, and HaPuR, and vanillate for VanA and VanB. Enzyme concentrations were as follows: 5 µM for AgcA and AgcB, 10 µM for VanA and VanB, 10 µM for PbdA, 5 µM for HaPuX, 1 µM for HaPuR, and 2.5 µM for SH. Gas mixtures containing 4% H_2,

20% O_2, and 76% N_2 were prepared and introduced into the vials following the same procedure described in Section 3.2. Briefly, gas was bubbled into the reaction mixture through a dual-needle setup, ensuring efficient equilibration between the liquid phase and the headspace. The bubbling process was maintained for 5 min at a total flow rate of 100 mL/min. To preserve the gas environment, needles were removed sequentially, starting with the venting needle, before sealing the vials with gas-tight butyl rubber septa and aluminum caps. Reactions were initiated by injecting enzyme solutions into the vials using a gas-tight Hamilton syringe, and the vials were incubated at 30 °C with continuous shaking at 200 rpm to ensure proper mixing and gas-liquid equilibrium. Sampling was performed at the endpoint after 16 h of incubation. Aliquots of 50 µL were withdrawn from each vial, immediately quenched 1:1 with 100% acetonitrile (LC-MS grade) to terminate the reaction, and placed on ice to minimize any post-reaction activity. Quenched samples were centrifuged at 12,000 × *g* for 10 min at 4 °C to remove precipitated proteins, and the clarified supernatants were transferred to HPLC vials equipped with glass inserts to ensure accurate analysis. HPLC analysis was conducted using the methods described previously, with a Macherey-Nagel NUCLEODUR C18 Gravity column (75 mm length, 4.6 mm inner diameter, 3 µm particle size) and a gradient elution program. The mobile phase consisted of water with 0.1% formic acid and acetonitrile with 0.1% formic acid, transitioning from 95% water and 5% acetonitrile to 95% acetonitrile over 20 min at a flow rate of 1 mL/min. UV detection was performed at 254 nm, 280 nm, 290 nm, and 320 nm.

3.4.2 Additional Results and HPLC Chromatograms

Table S4: Reaction mass efficiencies of H_2-driven O-demethylations under different NAD^+ concentrations

Enzymes	NAD^+ [mM]	RME [%][a]
AgcAB	0.1	15.7
AgcAB	0.2	21.6
AgcAB	0.3	26.9
AgcAB	0.4	26.5
PbdA/HaPuXR	0.1	15.9
PbdA/HaPuXR	0.2	25.4
PbdA/HaPuXR	0.3	27.1
PbdA/HaPuXR	0.4	26.8
VanAB	0.1	21.4
VanAB	0.2	21.7
VanAB	0.3	21.4
VanAB	0.4	21.2

[a] Reaction mass efficiencies (RME) was calculated as ($m_{product}/m_{reagents}$)

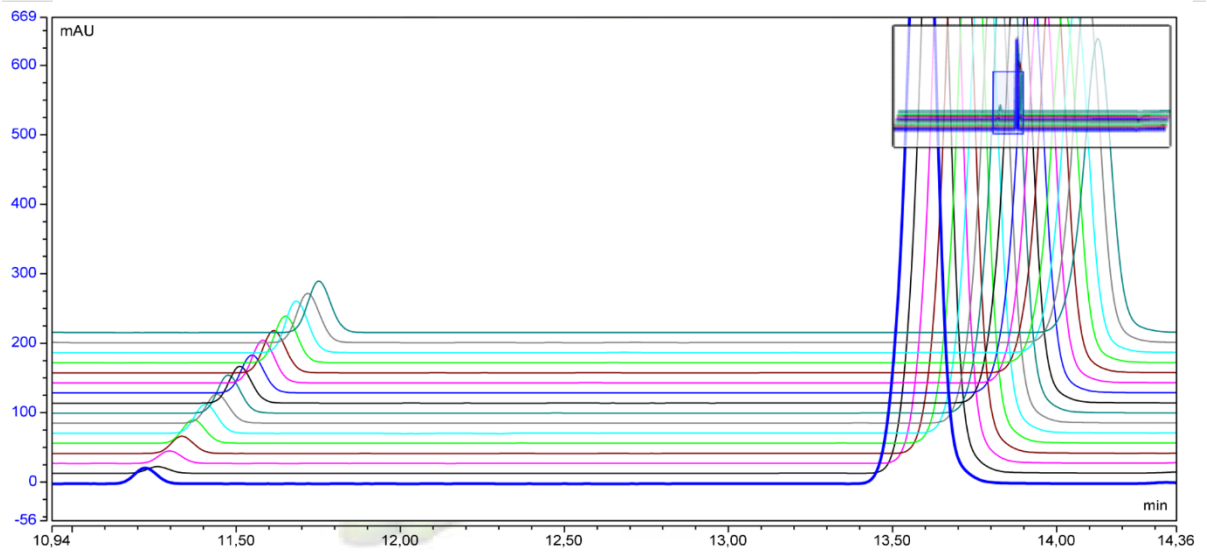

Fig. S5. HPLC chromatograms depicting the time-course conversion of ethylguaiacol (RT 13.6 min) to ethylcatechol (RT 11.0 min) catalyzed by AgcAB, with NAD^+ at a concentration of 0.1 mM.

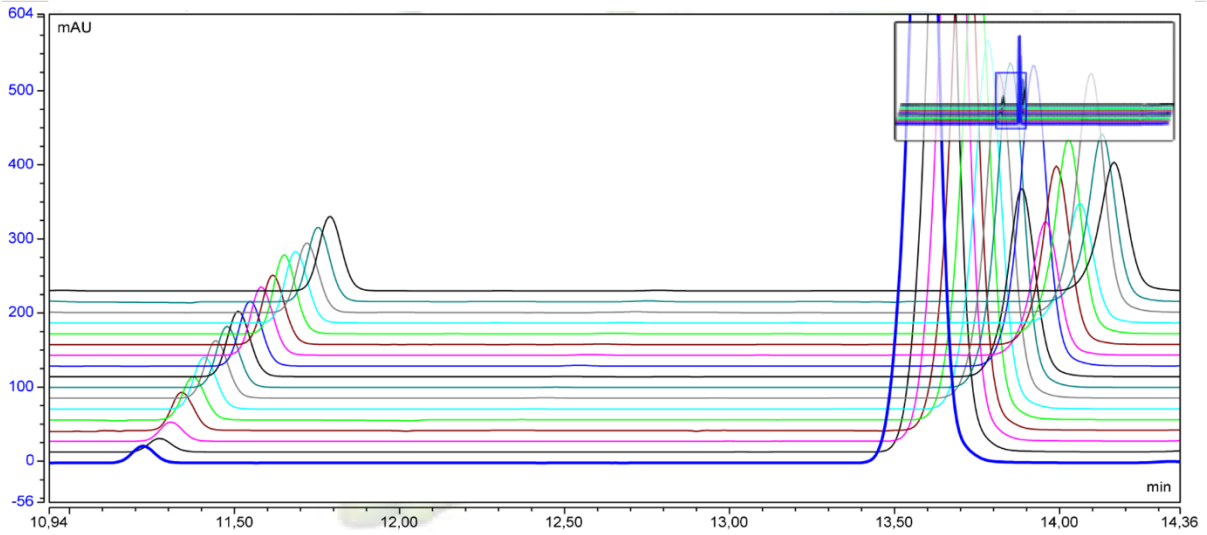

Fig. S6. HPLC chromatograms depicting the time-course conversion of ethylguaiacol (RT 13.6 min) to ethylcatechol (RT 11.0 min) catalyzed by AgcAB, with NAD^+ at a concentration of 0.2 mM.

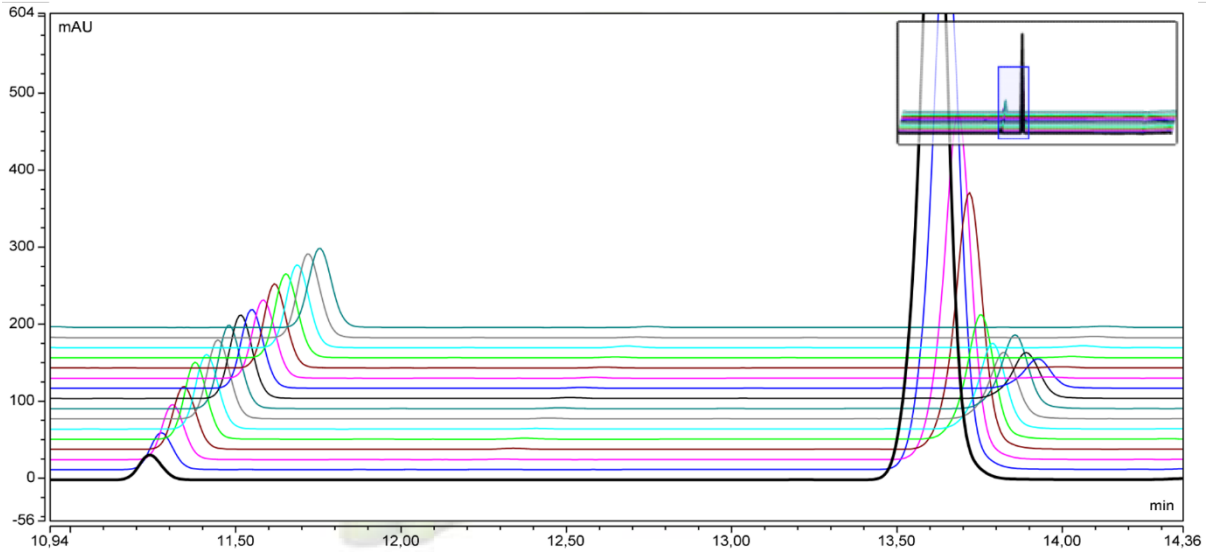

Fig. S7. HPLC chromatograms depicting the time-course conversion of ethylguaiacol (RT 13.6 min) to ethylcatechol (RT 11.0 min) catalyzed by AgcAB, with NAD^+ at a concentration of 0.3 mM.

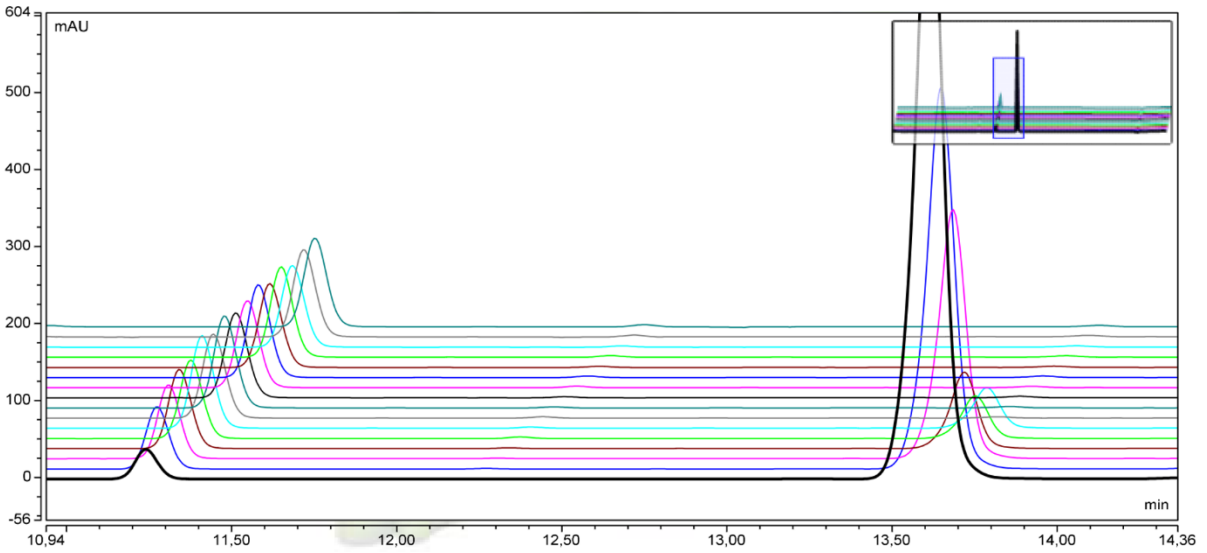

Fig. S8. HPLC chromatograms depicting the time-course conversion of ethylguaiacol (RT 13.6 min) to ethylcatechol (RT 11.0 min) catalyzed by AgcAB, with NAD^+ at a concentration of 0.4 mM.

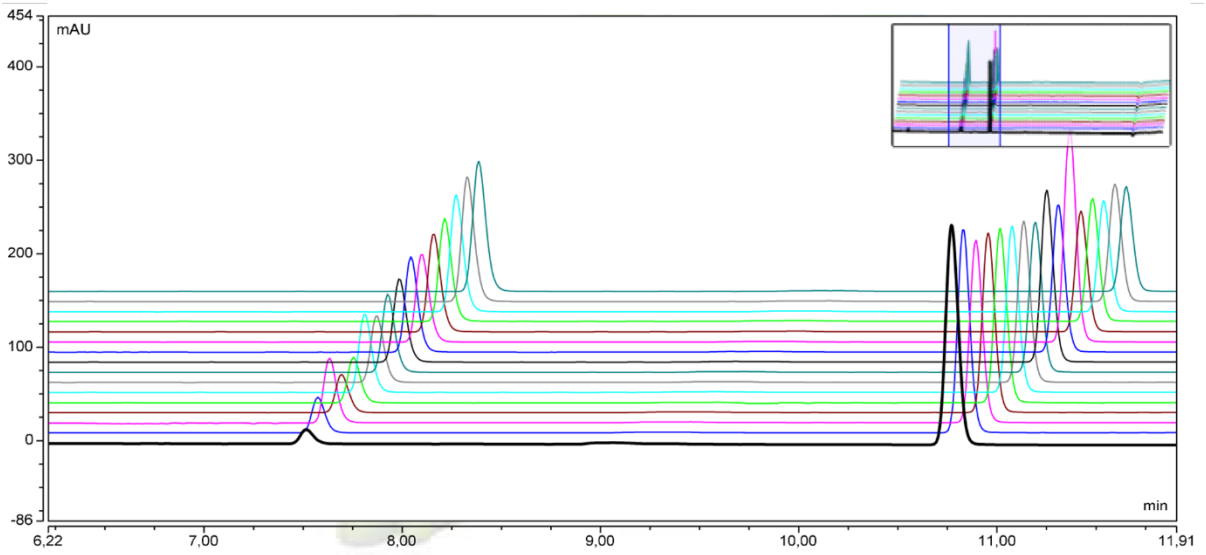

Fig. S9. HPLC chromatograms depicting the time-course conversion of p-methoxybenzoate (RT 10.8 min) to hydroxybenzoate (RT 7.6 min) catalyzed by PbdA/HaPuXR, with NAD^+ at a concentration of 0.1 mM.

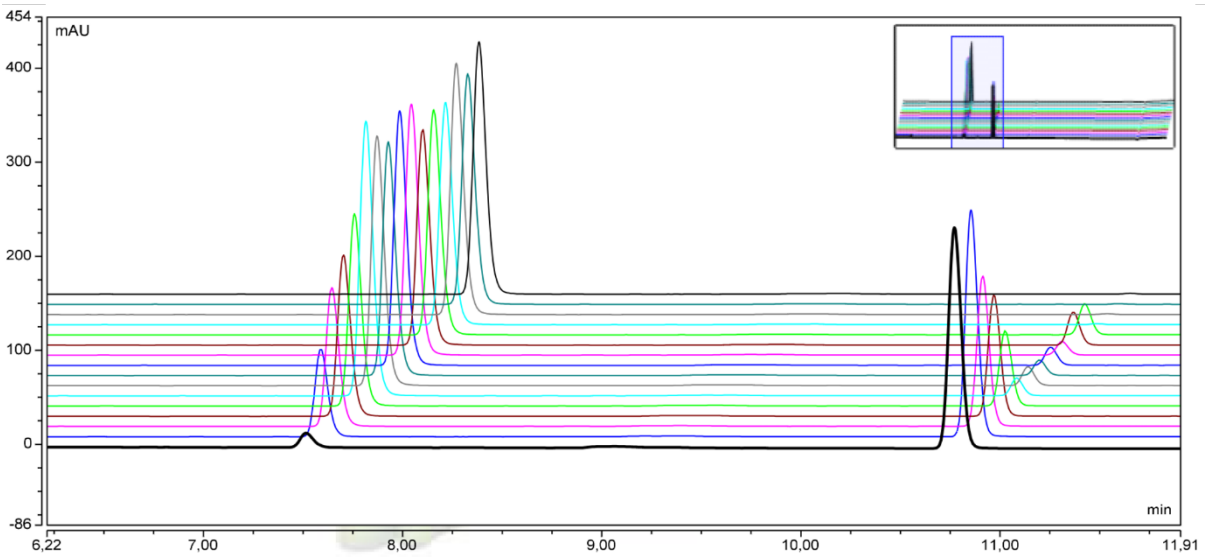

Fig. S10. HPLC chromatograms depicting the time-course conversion of p-methoxybenzoate (RT 10.8 min) to hydroxybenzoate (RT 7.6 min) catalyzed by PbdA/HaPuXR, with NAD^+ at a concentration of 0.2 mM.

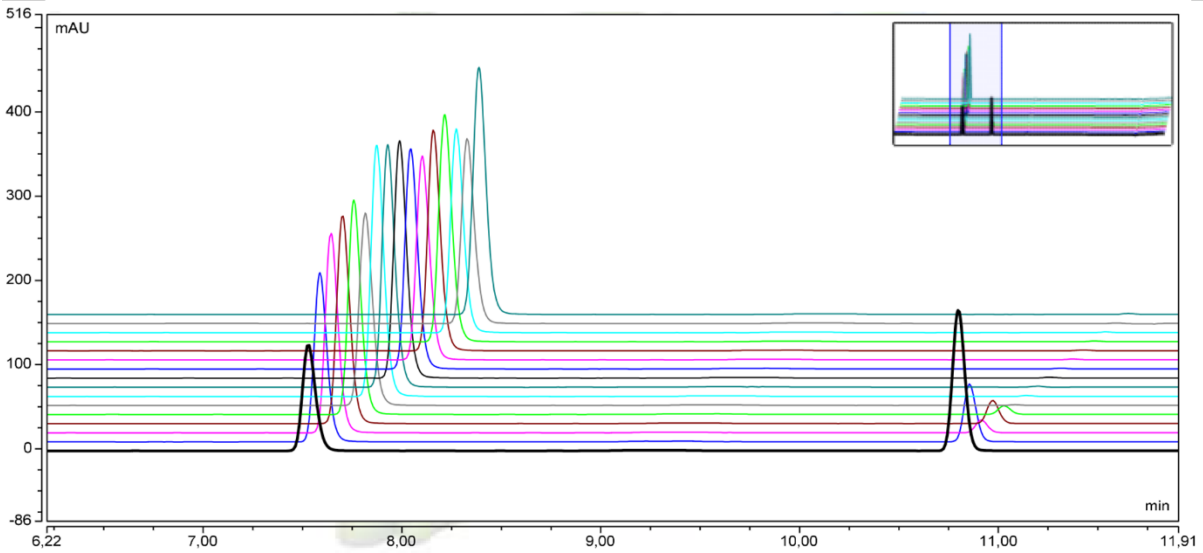

Fig. S11. HPLC chromatograms depicting the time-course conversion of p-methoxybenzoate (RT 10.8 min) to hydroxybenzoate (RT 7.6 min) catalyzed by PbdA/HaPuXR, with NAD^+ at a concentration of 0.3 mM.

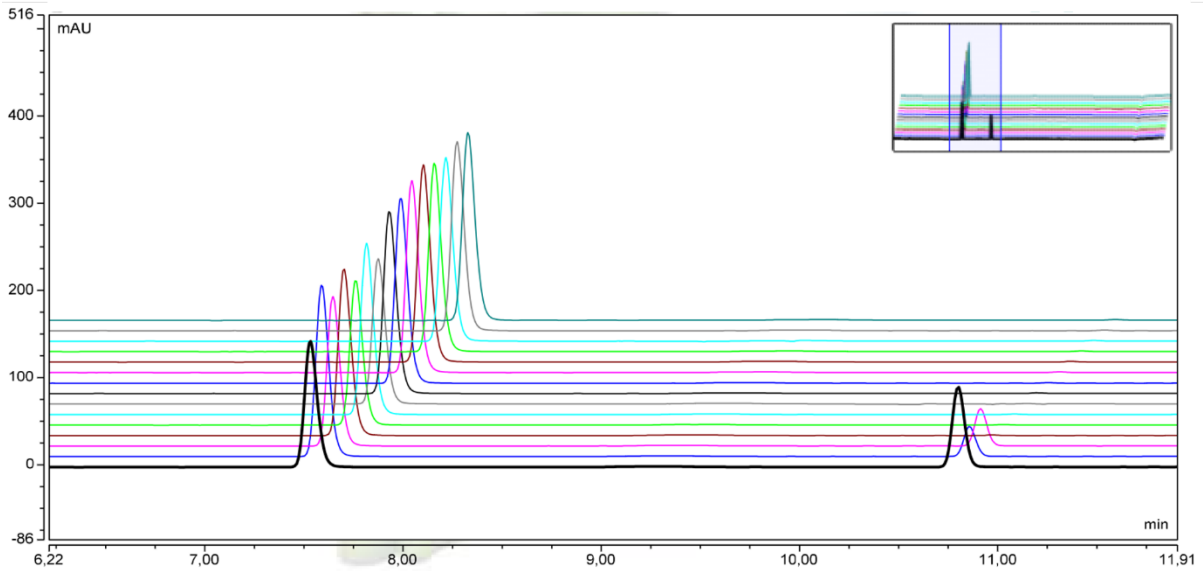

Fig. S12. HPLC chromatograms depicting the time-course conversion of p-methoxybenzoate (RT 10.8 min) to hydroxybenzoate (RT 7.6 min) catalyzed by PbdA/HaPuXR, with NAD^+ at a concentration of 0.4 mM.

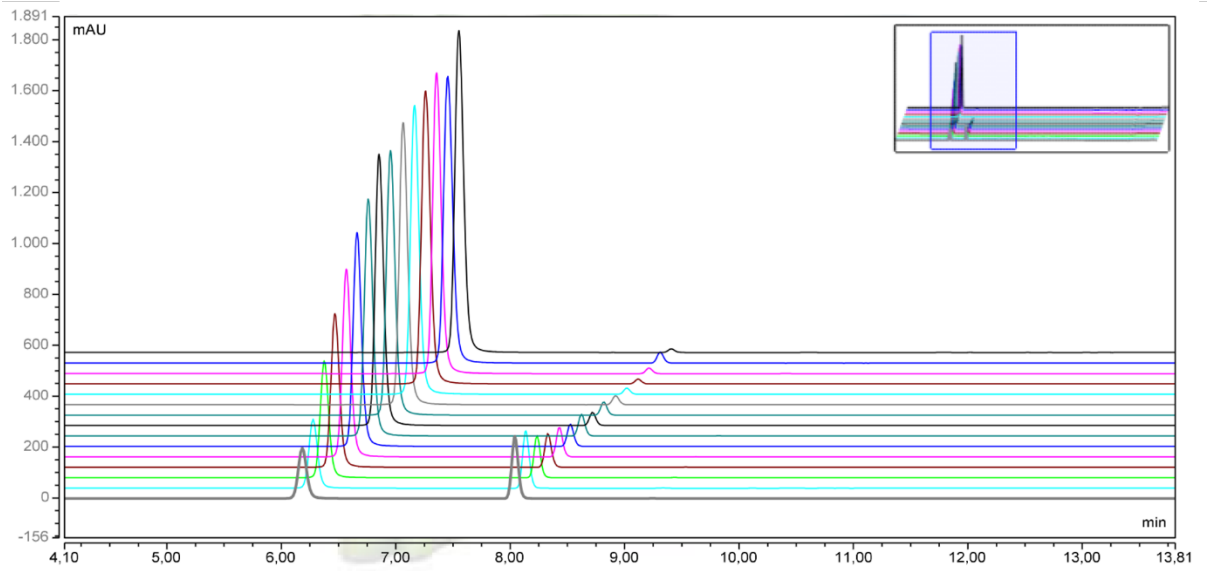

Fig. S13. HPLC chromatograms depicting the time-course conversion of vanillate (RT 8.05 min) to protocatechuate (RT 6.15 min) catalyzed by VanAB, with NAD^+ at a concentration of 0.1 mM.

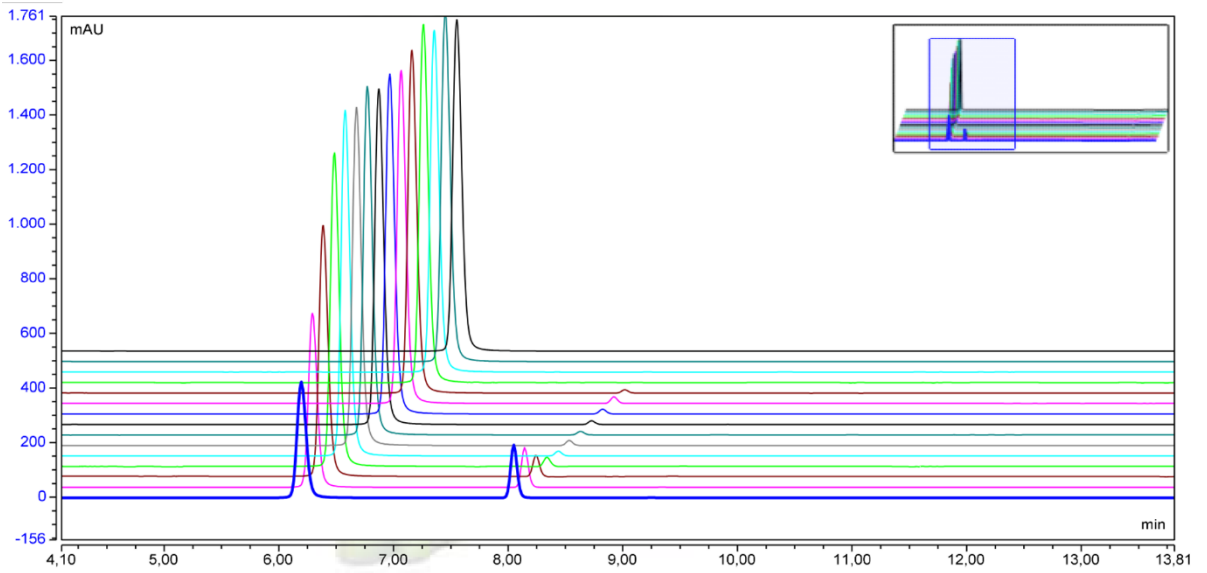

Fig. S14. HPLC chromatograms depicting the time-course conversion of vanillate (RT 8.05 min) to protocatechuate (RT 6.15 min) catalyzed by VanAB, with NAD^+ at a concentration of 0.2 mM.

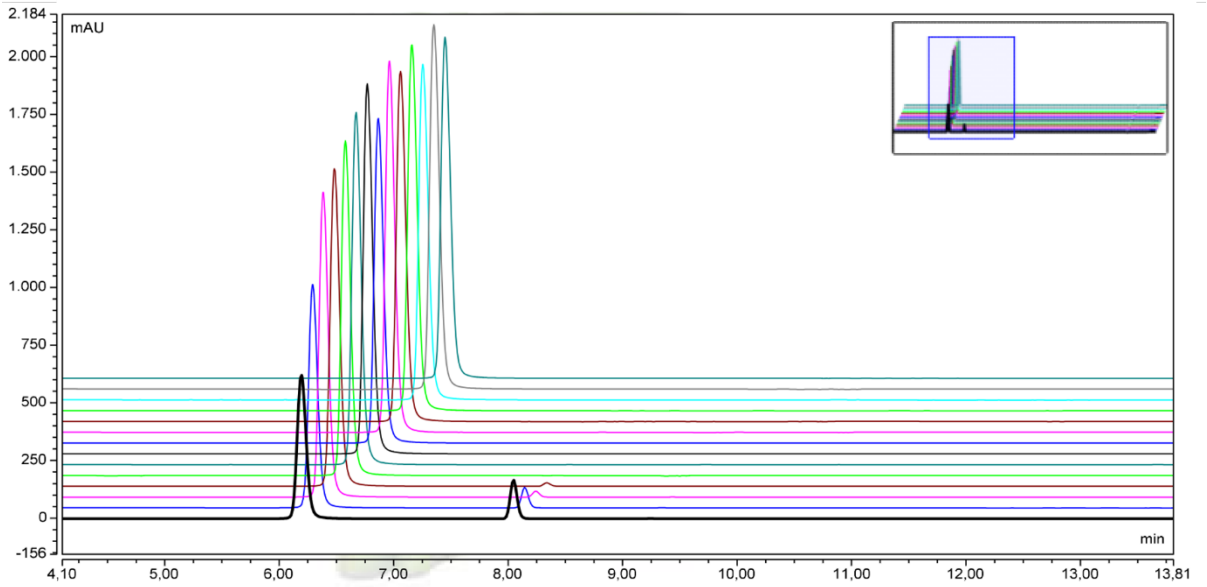

Fig. S15. HPLC chromatograms depicting the time-course conversion of vanillate (RT 8.05 min) to protocatechuate (RT 6.15 min) catalyzed by VanAB, with NAD^+ at a concentration of 0.3 mM.

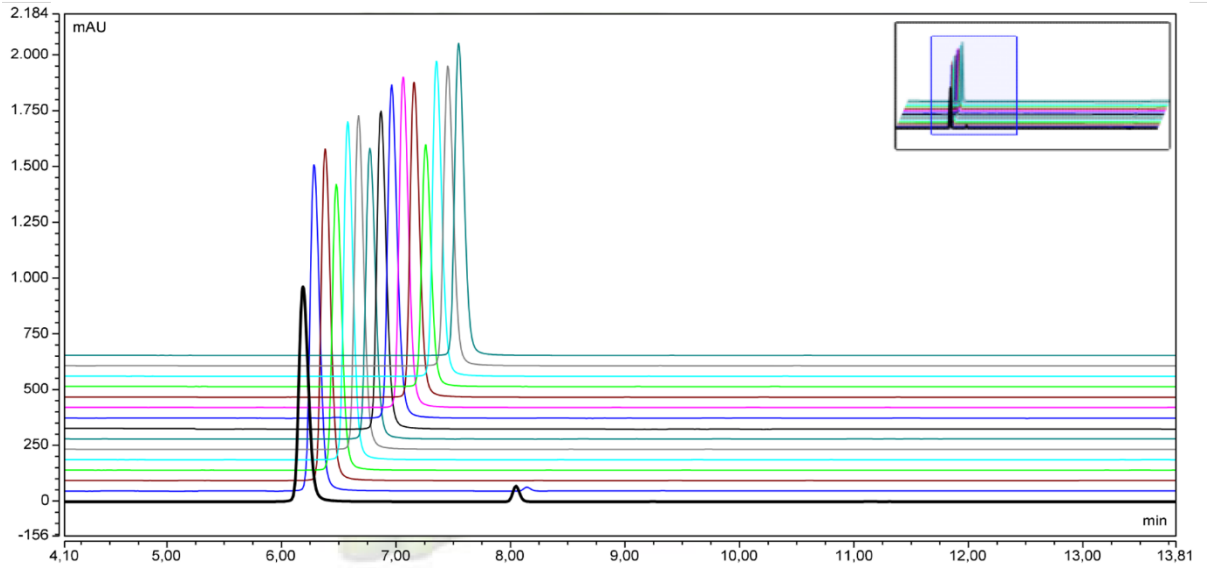

Fig. S16. HPLC chromatograms depicting the time-course conversion of vanillate (RT 8.05 min) to protocatechuate (RT 6.15 min) catalyzed by VanAB, with NAD^+ at a concentration of 0.4 mM.

3.5 UV-VIS kinetics analysis

Enzyme activity was analyzed using UV-Vis spectroscopy to monitor the consumption of NADH and the reduction of NAD^+. All measurements were conducted at 365 nm, the absorbance maximum of NADH, using a spectrophotometer equipped with a temperature-controlled cell holder and standard 1 cm quartz cuvettes. The reaction mixtures were prepared in 50 mM potassium phosphate, pH 7.5, with a total volume of 1 mL. The specific composition of the reaction mixture depended on the enzyme being analyzed but followed a consistent framework for both assays. For the NADH consumption assay, NADH was used as the electron donor at a final concentration of 400 µM. The reaction was initiated by the addition of the enzyme, which was included at a concentration adjusted based on its activity, typically ranging from 0.5 to 5 µM. Substrates specific to each enzyme, such as aldehydes for oxidoreductases, were added at the desired concentrations prior to the start of the reaction. A representative NADH consumption assay is shown in Fig. S16, where the time-dependent decrease in absorbance at 365 nm is highlighted.

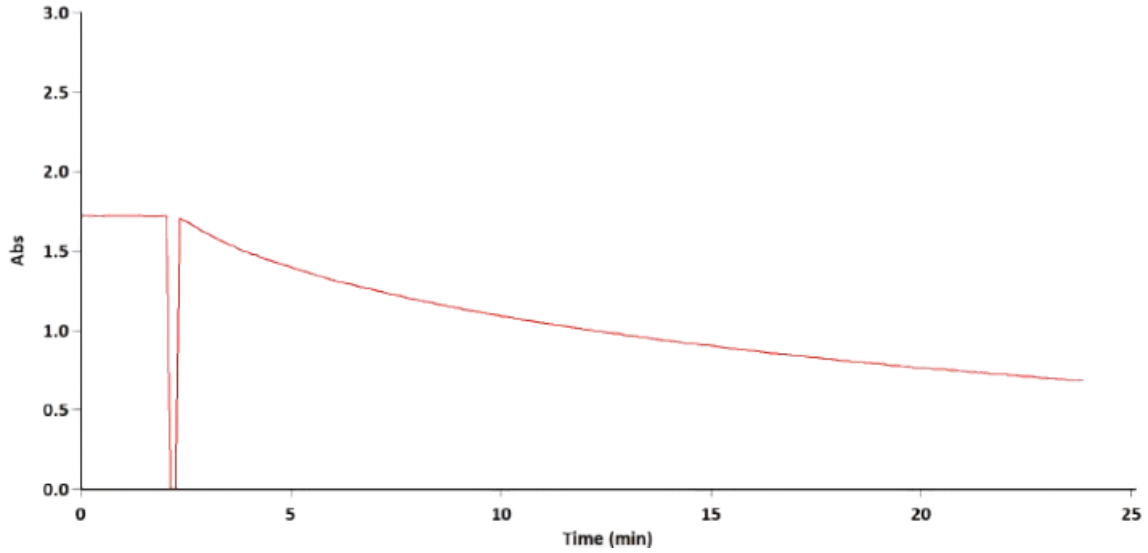

Fig. S17. UV-Vis kinetic spectrum illustrating the oxidation of NADH catalyzed by AgcAB. The activity was determined by calculating the initial slope of the absorbance decrease at 365 nm over time.

In the NAD^+ reduction assay, NAD^+ was included in the reaction mixture at a final concentration of 400 µM, along with an electron donor appropriate for the enzyme under study. For instance, formate was used for formate dehydrogenase (FDH), while hydrogen gas was supplied as the electron source for soluble hydrogenase (SH). Both SH and FDH, were added last to initiate the reaction, at a final concentration of 1 µM, ensuring the mixture was thoroughly mixed by gentle pipetting. The results of a representative NAD^+ reduction assay are presented in Fig. S17, which also includes the initial slopes used for calculating the reaction rates. Absorbance at 365 nm was recorded immediately after enzyme addition at 5-second intervals for a period of 3 to 5 min to capture the linear phase of the reaction. Blank reactions were prepared for each assay condition without the enzyme to account for any non-enzymatic changes in absorbance. The rate of NADH oxidation or NAD^+ reduction was determined from the slope of the linear portion of the absorbance versus time curve, using the extinction coefficient of NADH at 365 nm (ε = 3400 M^{-1} cm^{-1}). All measurements were performed in triplicate.

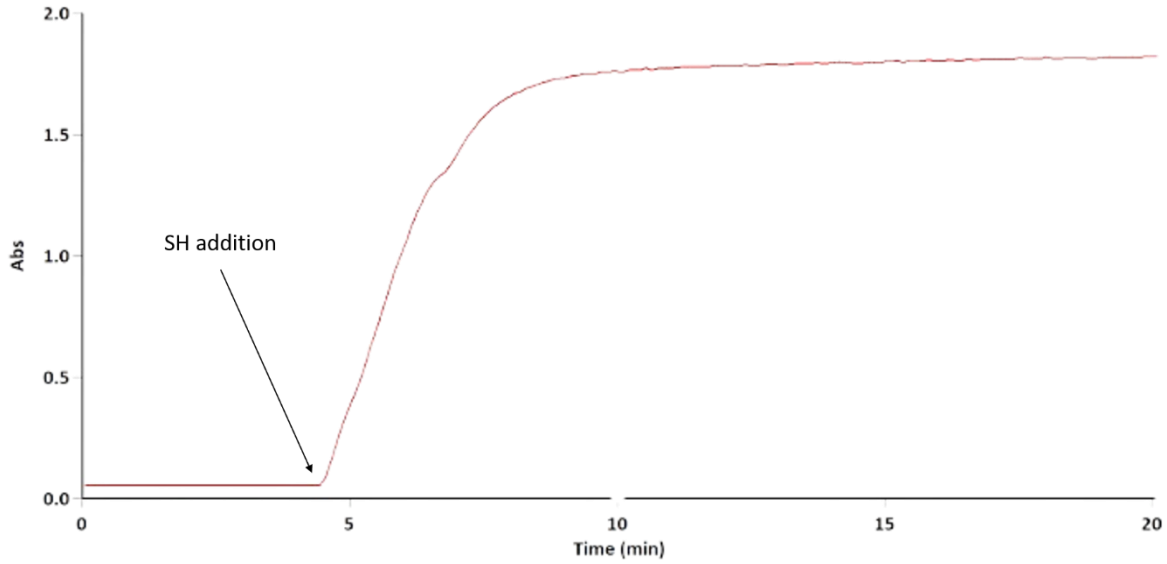

Fig. S18. UV-Vis kinetic spectrum illustrating the reduction of NAD^+ to NADH catalyzed by soluble hydrogenase (SH). The activity was determined by calculating the initial slope of the absorbance increase at 365 nm over time.

3.6 Electro-driven biotransformation with immobilized enzymes

3.6.1 Enzymes immobilization

Fig. S19. NADH regeneration unit consisting of a column packed with amberlite resin, on which soluble hydrogenase (SH) and catalase were immobilized for cofactor regeneration.

The immobilization process was carried out as follows: Amberlite FPA54 resin (4 g) was packed into a C 10/10 column and equilibrated by washing with five column volumes (5 CV) of 20 mM Tris-HCl buffer at pH 8. Soluble hydrogenase (SH) was immobilized on the resin by loading 4.5 mg of enzyme, scaled for a 200 mL reaction. VanA and VanB were not immobilized but were entrapped within a 3.5 kDa dialysis membrane, which was placed in a Schott glass reactor unit designed for biotransformation. A magnetic stir bar was added to the reactor, and the unit was maintained on a magnetic stirrer-hotplate at 60 rpm and 30 °C to ensure proper mixing. Catalase was included directly within the biotransformation unit, serving as a free enzyme to complement the reaction system. This configuration ensured efficient NADH regeneration and facilitated downstream biotransformation processes.

3.6.2 Continuous flow setup

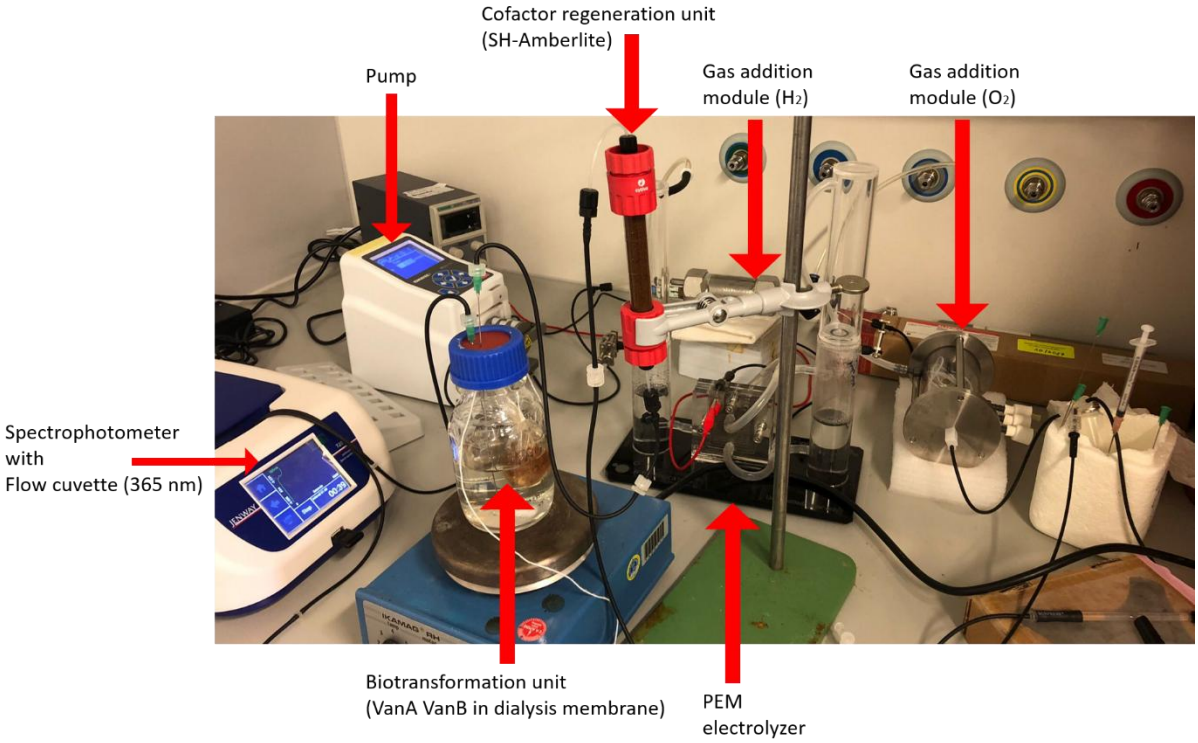

Fig. S20. Continuous closed-loop flow setup with integrated sensors, gas addition modules, biotransformation unit, spectrophotometer and PEM electrolyzer.

Two gas addition modules one encased in steel and the other encased in polyethylene were designed to facilitate the safe transfer of H_2/O_2 gas-to-liquid in the flow system. H_2 and O_2 gas addition module contained 2 m of PVMS (polyvinylsiloxane) tubing and 1 m of PTFE (polytetrafluoroetylene) tubing to add specific safe amount of H_2/O_2 mixture to the flow volume. To introduce H_2/O_2 to the gas addition modules from the PEM electrolzyer, IQS adapters equipped with mini ball valve were connected to allow pressurized conditions. Pressure gauge was also equipped measure pressure within the gas addition modules. Gas addition modules were equipped with a 1/4-28 and 10-32 adapter to be connected to the flow system. To ensure no contamination of atmospheric gas is permeated through the tubes outside the gas addition module during the reaction, Fluran® F-5500-A tubing with very low gas permeability was used throughout the flow setup. To add a specific amount of H_2/O_2 mixture into the flow setup, the gas addition modules were sequenced subsequently in the closed-loop flow setup. Despite that putting the O_2 gas addition module in front of the cofactor regeneration unit will optimize

the process, safe and precise amount gas addition was more important, therefore the two gas addition modules were subsequently put together and optimized before the reaction. Due to the tolerance of SH to O_2, certain amount of O_2 did not hinder the reaction. The amount of dissolved H_2, dissolved O_2 and temperature were measured on-line through an integrated flow sensor to understand the interplay of electrocatalysts and biocatalysts. Modified Clark-type H_2 sensor (UNISENSE) was integrated to the flow setup to measure dissolved H_2. Optical O_2 sensor (PreSens) was integrated with a cuvette attached with an adhesive O_2 spot to measure dissolved O_2. Rubber septa was inserted over the cuvette, to inhibit any atmospheric air while allowing substrate addition. Redox state of NAD^+/NADH was measured spectrophotometrically at 365 nm wavelength with a flow cuvette on-line during the reaction. The flow rate was constantly set to 3 mL min^{-1} to emulate gravity flow rate for SH-Amberlite, unless stated otherwise.

3.6.3 Formaldehyde derivatization and GC analysis

Detailed Methods

Formaldehyde in the samples was analyzed over time by collecting 50 µL of the reaction mixture at each time point. The collected samples were immediately derivatized with 2,4-dinitrophenylhydrazine (DNPH) to stabilize formaldehyde for subsequent analysis. The derivatization was carried out by adding 100 µL of DNPH solution, prepared in 2 M hydrochloric acid, to the 50 µL sample. The mixture was vortexed thoroughly for 10–15 seconds to ensure proper mixing and allowed to react at room temperature for 15 min, during which formaldehyde was converted into its hydrazone derivative. Following the reaction, 150 µL of methanol was added to stabilize the sample and reduce viscosity. The mixture was centrifuged at 14,000 rpm for 5 min to remove any particulates, and the clear supernatant was transferred to GC vials equipped with inserts for analysis. The derivatized samples were analyzed using a gas chromatograph equipped with a flame ionization detector (GC-FID). A ZB-Waxplus column (30 m × 0.25 mm × 0.25 µm) was employed for separation. The GC oven was programmed to hold at 60 °C for 5 min, followed by a gradient increase of 15 °C per min to a final temperature of 240 °C, which was held for an additional 5 min. The injector temperature was set to 250 °C, and the detector temperature was maintained at 300 °C. Helium was used as the carrier gas at a flow rate of 1 mL/min, and 1 µL of the sample was injected in 1:10 split mod. Formaldehyde concentrations were determined by integrating the chromatographic peak areas corresponding to the formaldehyde hydrazone derivative and comparing these values to a calibration curve constructed using known concentrations of formaldehyde derivatized under identical conditions.

Additional Results and GC Chromatograms

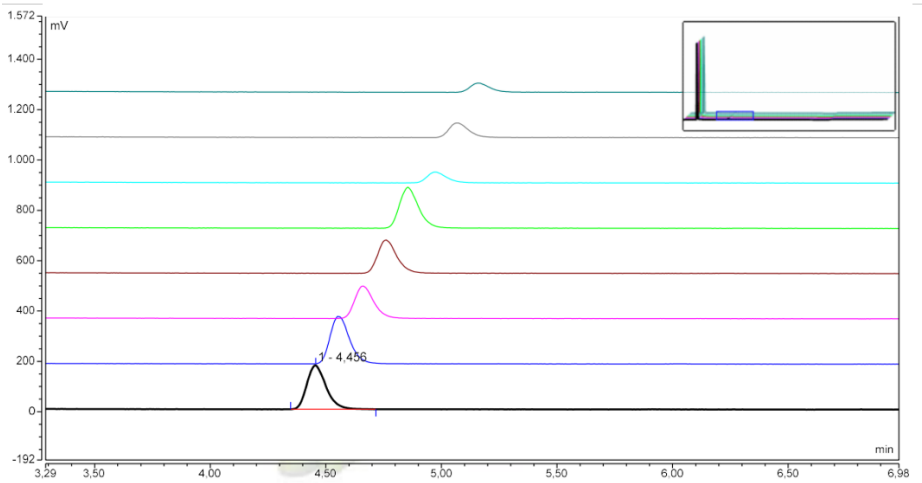

Fig. S21. Gas chromatograms illustrating the time-course profiles of DNPH-derivatized formaldehyde, analyzed via GC-FID.

3.6.4 Yields, downstream processing and extraction

Samples were taken at regular intervals to monitor the reaction progress. Small aliquots were collected for analysis via TLC, HPLC, and GC. For TLC, pre-coated TLC sheets (Alugram Sil G) were used to assess product formation qualitatively on-line, while HPLC was employed to quantify substrate conversion, and GC was used to measure formaldehyde concentration. Sampling continued until TLC indicated complete conversion. The yields over time are shown in Fig. S21.

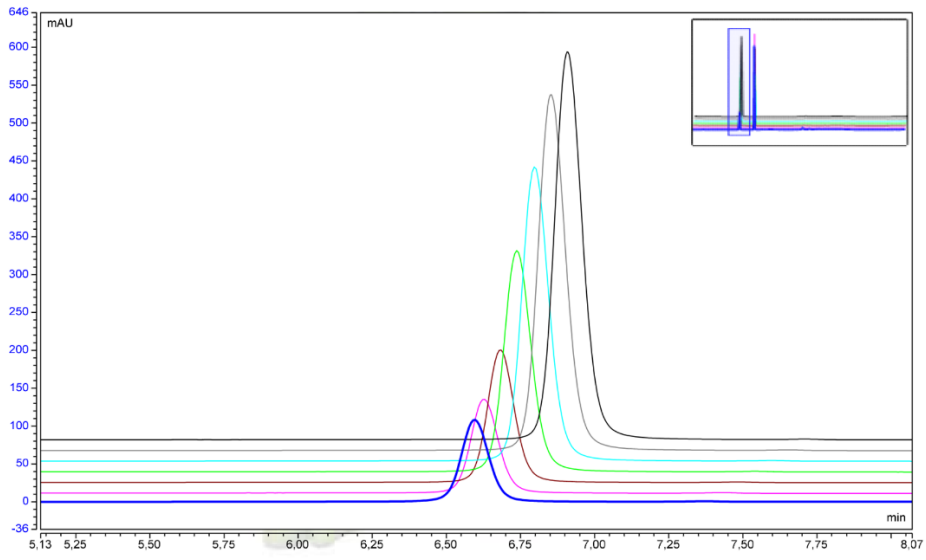

Fig. S22. HPLC chromatograms illustrating the time-dependent accumulation of protocatechuate catalyzed by VanA/VanB in the flow setup.

After the reaction, the NADH regeneration unit was detached, and the dialysis membrane was removed. The product retained in the dialysis membrane was recovered by immersing the membrane in 1 L of distilled water overnight to ensure complete diffusion of the product. The dialysis membrane

was then discarded. The entire flow reaction medium, along with the contents recovered from the dialysis membrane, was extracted twice using ethyl ether. The combined organic phases were dried over anhydrous sodium sulfate and concentrated under reduced pressure. The crude product was then crystallized and subjected to further characterization by NMR, and the spectrum is presented in Fig. S22, confirming the purity and identity of the product.

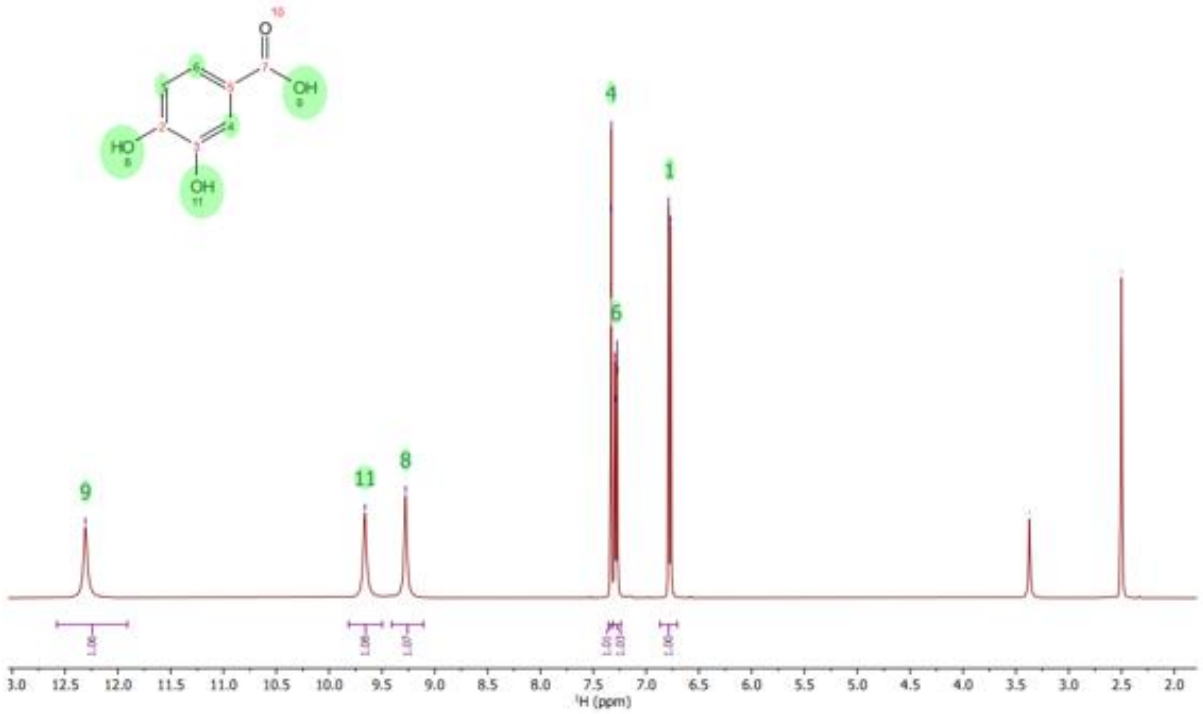

Fig. S23. ^{1}H NMR spectrum of the purified product obtained from the flow setup.

4 Faraday efficiency

(1) $$Faradaic\ efficiency\ (\%) = \frac{Actual\ electrons\ used}{Total\ electrons\ passed} = \frac{\alpha n F}{Q} \times 100$$

$\alpha =$ molar yield of the desired product (mol)
$n =$ electrons needed (n = 2)
$F =$ Faraday constant (96485 C mol^{-1})
$Q =$ total charges passed during the reaction as H_2 gas (current (A) x time (s))

Faradaic efficiency of the continuous flow system coupled with a commercial PEM electrolyzer was determined with an electro-driven *O*-demethylation from **vanillate** to **protocatechuate**. NAD^+ and substrate **vanillate** were added to achieve concentrations of 0.3 mM and 50 mM, respectively. PEM electrolyzer (H-Tec education) was set to 3.9 V, 2.21 A (H_2 33 mL min^{-1}, O_2 16 mL min^{-1}) for 5 min as pulse electrolysis and turned off. After 3.8 h substrate addition, to ensure full conversion of substrate, PEM electrolyzer was set to 3.5 V, 1.03 A (H_2 21 mL min^{-1}, O_2 10 mL min^{-1}) for 1 hour. The Faradaic efficiency was calculated according to the Equation 1. The Faradaic efficiency of the continuous flow system until 4 h after substrate addition was calculated to 62.1 %. When including until 5 h after substrate, Faradaic efficiency was calculated to 18.7 %.

5 Environmental impact, *E*-factor, E^+-factor

(2) $$E = \frac{\sum_i Mass\ of\ waste_i}{\sum_j Mass\ of\ product_j} \left[\frac{kg}{kg}\right]$$

(3) $$E^+ = \frac{\sum_i Mass\ of\ waste_i}{\sum_j Mass\ of\ product_j} \left[\frac{kg}{kg}\right] + \frac{W \times CI}{m(product)} \left[\frac{kWh \times \frac{kg(CO_2)}{kWh}}{kg}\right]$$

E-factor was roughly calculated to estimate the environmental impact of the reaction (Equation. 2). E^+-factor was also calculated to compromise the CO_2-emissions caused by electricity generation. Average OECD value (2015) was used as 404 g_{CO2} kWh^{-1}. Vanillate to protocatechuate in 200 mL reaction was evaluated. W = electrical power used; CI = carbon intensity [Grid average EU, 0.4 (kg CO_2/kWh)].

Table S5. *CO_2 formation based on the energy demand during VanA, VanB and SH production*

Process	Entry[a]	Energy consumption [kWh]	CO_2 [b][kg]
SH production	Cultivation + concentration	9.6	3.8780
VanAB production	Cultivation + concentration	1.3	0.52
PEM electrolysis during reaction	3.9 V, 2.21 A, 5 min	0.0007	0.0003
	3.5 V, 1.03 A, 60 min	0.0036	0.0014

[a] By process, energy consumption is included by each steps during enzyme production: cultivation includes shaker of media, concentration includes ultracentrifugation of lysed enzyme, purification was done by gravity columns.
[b] Calculated based on 404 g CO_2 KWh^{-1} (OECD for Europe 2015)

Table S6. *E^+* factor for O-demethylation reaction in flow system

Reaction, volume	$Mass_{waste}$ components[a]	Waste (mg)	$Mass_{product}$ (mg) [b]	*E* factor	E^+-factor[c]
VanAB reaction driven by SH/H_2, 200 mL	Tris (20 mM)	485	1541	3.6	2846.9
	NAD^+ (0.3 mM)	39.8			
	Isolated SH	4.85			
	Isolated VanAB	6.5			
	Amberlite FPA54	4000			
	Dialysis membrane	1000			
	Catalase	10			

[a] Waste component were determined using Tris-HCl buffer at pH 8 (with indicated concentration). No side reactions were observed during this reaction. Mass from cultivation, purification step and H_2 gas were not included as waste components.
[b] The production of protocatechuate as a product was quantified.
[c] The E^+-factor furthermore takes energy demand and take into account the CO_2 emissions that comes from the energy that was used.

6 Carbon efficiency calculations

Carbon efficiency calculation of vanillate (4-hydroxy-3-methoxybenzoate) to protocatechuate (3,4-dihydroxybenzoate) is as follows (Vanillate → Protocatechuate + Formaldehyde):

(4) $$Carbon\ efficiency\ [\%] = \left(\frac{7}{8}\right) \cdot 100 = 87.5\ \%$$

This is calculated when formaldehyde is considered waste, formaldehyde can be reutilized or further used in cascade where the carbon efficiency can be higher.

7 EcoScale calculations

EcoScale is a semi-quantitative green chemistry metric (0-100) that penalizes non-ideal reaction features:

Parameter	Penalty points
1. Yield	0
2. Price of reaction components	3
3. Safety	0
4. Technical setup	1
5. Temperature/time	0
6. Workup and purification	14

Penalty points equal to 18, which comes to EcoScale 88 points.

8 Atom economy, atom efficiency calculations

(5) $$Atom\ economy\ (AE\ [\%]) = \left(\frac{\sum Molecular\ weight\ (MW) of\ desired\ product}{\sum MW\ of\ all\ reactants}\right) \cdot 100$$

By the molecular weight of all reactants it leads to vanillate (168.15 g/mol), H_2 (2 g/mol), O_2 (32 g/mol), protocatechuate (154.12 g/mol). It leads to 76.24 %

(6) $$Atom\ efficiency\ (AE\ f\ [\%]) = (AE \times \text{Yield})/100$$

With yield leading up to 99.5 %, the atom efficiency calculates to 76.16 %.

9 Formulas

(7) $$Activity\ (U) = \frac{\Delta Absorbance}{\Delta t} \cdot \frac{V_{total}}{\varepsilon \cdot l}$$

(8) $$Reaction\ Mass\ Efficiency\ (RME\ [\%]) = \left(\frac{\sum_i Mass\ of\ desired\ product_i}{\sum_j Mass\ of\ reactant_j}\right) \cdot 100$$

(9) $$Carbon\ efficiency\ [\%] = \left(\frac{Number\ of\ carbon\ atoms\ in\ desired\ product}{Total\ number\ of\ carbon\ atoms\ in\ all\ reactants}\right) \cdot 100$$

10 References

1. Fetherolf, M.M. et al. (2020) Characterization of alkylguaiacol-degrading cytochromes P450 for the biocatalytic valorization of lignin, *PNAS*, 117 (41), 25771-25778.
2. Notonier, S. et al. (2021) Metabolism of syringyl lignin-derived compounds in Pseudomonas putida enables convergent production of 2-pyrone-4,6-dicarboxylic acid, *Metab Eng*, 65, 111-122.
3. Wolf, M.E. et al. (2024) Characterization of a cytochrome P450 that catalyzes the *O*-demethylation of lignin-derived benzoates, *Journal of Biological Chemistry*, 107809.
4. Tieves, F., Tonin, F., Fernández-Fueyo, E., Robbins, J. M., Bommarius, B., Bommarius, A. S., Alcalde, M., & Hollmann, F. (2019). Energising the E-factor: The E + -factor. *Tetrahedron*, *75*(10), 1311–1314.
5. van Aken, K., Strekowski, L., & Patiny, L. (2006). EcoScale, a semi-quantitative tool to select an organic preparation based on economical and ecological parameters. *Beilstein Journal of Organic Chemistry 2:3*, *2*(1), 3.